Journal of Computational Applied Mechanics 2022, 53(1): 1-22

DOI: 10.22059/jcamech.2022.339008.693
RESEARCH PAPER

Dynamic analysis of functionally graded carbon nanotube (FGCNT) reinforced composite beam resting on viscoelastic foundation subjected to impulsive loading

Faraz Kiarasi[1], Ali Asadi[2], Masoud Babaei[1], Kamran Asemi[2,*], Mohammad Hosseini[3]

[1] *Department of Mechanical Engineering, University of Eyvanekey, Eyvanekey, Semnan, Iran.*

[2] *Department of Mechanical Engineering, Islamic Azad University, North Tehran Branch, Tehran, Iran.*

[3] *Department of Mechanical Engineering, University of Hormozgan, Bandar Abbas, Iran.*

Abstract

In this study, dynamic analysis of functionally graded carbon nanotube reinforced composite (FGCNT) beam resting on viscoelastic foundation is investigated. Four different types of carbon nanotubes (CNTs) distribution including uniform (UD-CNT), and three types of functionally graded distribution of CNTs through the thickness of beam are considered. The Kelvin–Voigt viscoelastic model and higher-order shear deformation beam theory (HOBT) have been used. The rule of mixture is used to describe the effective material properties of the nanocomposite beams. The equations of motion are derived by using Lagrange's equations, and solved by using finite element and Newmark methods. The effects of volume fraction and distribution of CNTs, stiffness and damping of viscoelastic foundation, slenderness ratio and different boundary conditions on transverse displacement and stresses of beam are investigated. The results show that by using viscoelastic foundation the amount of normal and shear stress have decreased considerably, and by increasing the stiffness coefficient of foundation, transverse displacement of beam reduces and the frequency of vibration increases as well, meanwhile by increasing the damping coefficient of foundation, amplitude of vibration decreases considerably. The model is verified and compared with previously published works and it shows good agreement.

Keywords: Type your keywords here, separated by semicolons;

1. Introduction

Analysis of dynamic behavior of structures is one of the applied topics in mechanical engineering that has occupied many researchers and engineers. One of the important of structural components is beam, which are mainly subjected to dynamic loads. The use of beams as the main components of structures in various fields, including aerospace, marine, civil engineering, etc., has been become very common. Geometric and mechanical characteristics of the beam, and its foundation are considered as some factors that have considerable effects on the dynamic response of the beam. Therefore, the type of materials used in the design of the beams is also important. Extensive research has been done on the static and dynamic behavior of composite and FGM beams. Shi and Elm [1] investigated the dynamic behavior of composite beams based on the third-order theory by using the finite element method. Sankar [2] proposed an analytical solution based on Euler-Bernoulli's theory for FGM beam under transverse fluctuating load. Chen and Hong [3] studied the free vibrations of the Timoshenko beam resting on a viscoelastic foundation under a moving oscillating load. They studied the effect of various parameters such as

* Corresponding author. *E-mail address:* k.asemi@iau-tnb.ac.ir

foundation stiffness, shear layer viscosity, load velocity and axial force on the dynamic response. Chakrabuty et al. [4] proposed a new finite element method based on the first-order shear deformation beam theory and used it to study the thermoelastic behavior of a FGM beam. Kargar Novin and Younesian [5] investigated the dynamic response of Timoshenko beam resting on a viscoelastic foundation under the moving load by employing an infinite mixed Fourier transform. Based on Euler-Bernoulli theory, Yang et al. [6] investigated the free vibrations of a cracked FGM beam by considering different boundary conditions under moving loads. Kadoli et al. [7] studied the static analysis of FGM beam based on the third-order shear deformation theory and the finite element method. Ying et al. [8] presented a close form solution for the free and static vibrations of a FGM orthotropic beam based on the theory of two-dimensional elasticity resting on elastic foundation. Klim [9] presented the dynamic response of FGM beams based on Timoshenko's beam theory resting on viscoelastic foundation by applying the Darbin solution method. Using the Euler-Bernoulli beam theory and the Newmark method, Sismak [10] studied the free and forced vibrations of the FGM beam subjected to moving harmonic load. In another work [11], by considering the shear deformation and nonlinear effects, He studied the FGM beam under the harmonic load and used the same method. Khalili et al. [12] analyzed the forced vibrations of a FGM beam subjected to a moving mass based on Euler-Bernoulli beam. The mixed of Ritz and DQM approaches were used to solve the governing equation of motion. Mohebpour et al. [13] employed FEM procedure to investigate the dynamic analysis of composite beams by considering the effects of rotational and shear inertia and using Newmark methods. Pradan and Chakrawardi [14] employed Ritz method studied the free vibrations of FGM beams based on the theory of Timoshenko and Euler Bernoulli. Abdolghani et al. [15] studied the dynamic response of Euler-Bernoulli beam resting on a nonlinear viscoelastic foundation under moving load. They used the Galerkin and Rang Kota methods to solve differential equations of motion.

In recent years, the use of low-weight and high-strength materials such as FGM and particularly nanocomposites, has attracted engineers and designers’ minds [16-38]. One of these materials is functionally graded carbon nanotube (FGCNT) [39-41]. The mechanical properties of carbon nanotubes, such as high modulus of elasticity and low density, make it a good choice for reinforcing polymer composites [42-50]. Due to these materials being widely applied in various practical applications and industries, it is very important to study the dynamic response of nanocomposite beams. Voight and Adley [51] investigated the transient deflection and stress of composite beams reinforced with CNT based on Eluer-Bernoli theory. They found that the stiffness of these beams was significantly increased by applying a low volume fraction of nanotubes with a uniform distribution. Vednitcherova and Zang [52] presented an analytical solution for bending and buckling of FGCNT reinforced composite beams based on Eluer-Bernoli theory. Koh et al. [53] employed Ritz method to study the nonlinear analysis of free vibrations of FGCNT Timoshenko beam with linear and nonlinear distribution of CNT in the direction of thickness. Yas and Heshmati [54] investigated the dynamic analysis of FGCNT reinforced composite beams under moving load based on Timoshenko and Euler–Bernoulli beam theories. In order to model the material properties of composite beams reinforced with carbon nanotubes, the Mori Tanaka model was used. They investigated the effect of nanotube orientation, material distribution, moving load velocity and different boundary conditions on the vibration analysis of the beam. Shen and Yang [55] studied free vibrations, nonlinear bending, and post-buckling of beams made of FGCNT reinforced composites resting on an elastic foundation based on higher order shear deformation theory under thermal conditions. He and his colleagues [56] investigated the dynamic stability of beams made of FGCNT reinforced composite beam. The governing equations were extracted based on the first-order shear theory and converted to a linear equation system using the squares difference method. Then the effect of various factors such as volume fraction of carbon nanotubes, length to thickness ratio and boundary conditions on the dynamic stability of the beam was studied. Ansari et al. [57] studied the forced nonlinear vibrations of FGCNT reinforced composite Timoshenko beam by applying GDQM. Lin and Young [58] analyzed the free vibrations of FGCNT reinforced composite beams with various boundary conditions based on the first- and third-order shear theory and the Ritz method. Chahadhari et al. [59] presented a nonlinear analytical solution for the free vibrations of FG CNT reinforced composite beam with different boundary condition based on the high order of shear theory resting on an elastic foundation in thermal environments.

A review of the studies shows that most of the researches have been done so far on FGCNT beams are focused on static and free vibrations responses. But the transient vibrations of these beams have not been studied. Also, the effect of viscoelastic foundation on the dynamic response of carbon Nano type-reinforced beams has not been investigated among published investigations. This research investigates the dynamics response of FGCNT reinforced composite beams resting on a viscoelastic foundation based on high-order (third-order) beam theory. The finite element method in conjunction with Lagrange equation and Newmark method are applied to solve the governing equations of FGCNT reinforced composite beam. The existing papers by applying simplification are used for validation in the present work.

2. Theoretical formulations

2.1 Description of the Geometry:

An FGCNT beam with thickness h, length L and depth b is considered in Fig 1.

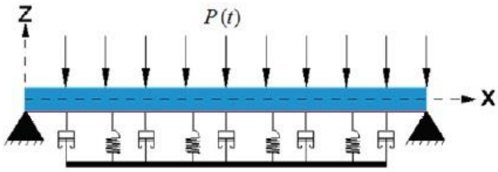

Fig 1: Description of geometry and coordinate system of FGCNTRC beam

2.2 Material properties of CNTRC:

The carbon nanotubes are considered to have uniform or FG distributions in the beam thickness. UD-CNTRC denotes the uniform distribution of CNTs and FGX, FGO and FGV-CNTRC show the FG patterns of CNTs through the beam thickness (Fig. 2). The effective mechanical properties of beam, mixtures of isotropic polymeric matrix and CNTs are evaluated by using the rule of mixtures as [60]:

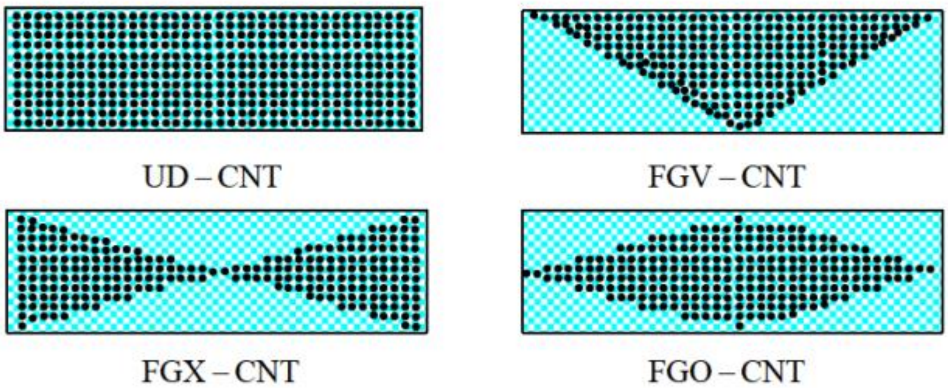

Fig 2: Different kinds of CNTs distribution

$$\rho = V_{CN}\rho^{CN} + V_m\rho^m$$

$$E_{11} = \eta_1 V_{CN} E_{11}^{CN} + V_m E^m \tag{1}$$

$$\frac{\eta_2}{E_{22}} = \frac{V_{CN}}{E_{22}^{CN}} + \frac{V_m}{E^m} \quad , \quad \frac{\eta_3}{G_{12}} = \frac{V_{CN}}{G_{12}^{CN}} + \frac{V_m}{G^m}$$

$$\upsilon_{12} = V_{CN}\upsilon_{12}^{CN} + V_m\upsilon^m \tag{2}$$

where E_{11}^{CN}, E_{22}^{CN}, G_{12}^{CN}, υ_{12}^{CN} are modulus of elasticity, shear modulus and Poisson's ratio of carbon nanotubes, respectively. Also, E^m, G^m and υ^m are the same properties of isotropic polymer matrix. ρ^m and ρ^{CN} are the mass density of matrix and CNTs, respectively. V_{CN} is the volume fraction of CNTs, and V_m is the volume fraction of polymer matrix ($V_{CN} + V_m$=1). V_{CN} for different distribution of CNTs are shown in Table 1. CNTs efficiency parameters $\eta_i, i = 1,2,3$ are given in Table 2 [61].

Table 1. Mathematical representation of CNT distributions

CNTs distribution	V_{CN}
UD CNT	V_{CN}^*
FG- X CNT	$4V_{CN}^* \frac{\|z\|}{h}$
FG- V CNT	$V_{CN}^* (1 + 2\frac{\|z\|}{h})$
FG- O CNT	$2V_{CN}^*(1\text{-}2\frac{\|z\|}{h})$

Table2. CNTs efficiency parameters for different values of V_{CN}^*

Efficiency parameter	V_{CN}^*=0.11	V_{CN}^*=0.14	$V_{CN}^* = 0.17$
η_1	0.149	0.150	0.149
η_2	0.934	0.941	1.381
η_3	0.934	0.941	1.381

3. Governing equation

3.1. Displacement field and strain

The displacement field based on the third-order beam theory of Reddy [62-66] is given by:

$$u(x,z,t) = u_0(x,t) + z\Phi_x(x,t) - 4\frac{z^3}{3h^2}\left[\Phi_x(x,t) + \frac{\partial w_0(x,t)}{\partial x}\right] \tag{3}$$

$$w(x,z,t) = w_0(x,t) \tag{4}$$

where u and w are the displacement components in the x and z directions, respectively. u_0 and w_0 are the mid-plane displacements and Φ_x is the bending rotation of x-axis. t denotes time and h is the total thickness of the beam. The matrix form of the displacement field is as:

$$\bar{u} = \begin{bmatrix} u \\ w \end{bmatrix} = \begin{bmatrix} 1 & 0 & -4\frac{z^3}{3h^2} & (z - 4\frac{z^3}{3h^2}) \\ 0 & 1 & 0 & 0 \end{bmatrix} \begin{bmatrix} u_0 \\ w_0 \\ \frac{\partial w_0}{\partial x} \\ \Phi_x \end{bmatrix} = [Z_c]\ [\bar{U}] \tag{5}$$

where

$$[\bar{U}] = \begin{bmatrix} u_0 \\ w_0 \\ \frac{\partial w_0}{\partial x} \\ \Phi_x \end{bmatrix}$$

$$[Z_c] = \begin{bmatrix} 1 & 0 & -4\frac{z^3}{3h^2} & (z - 4\frac{z^3}{3h^2}) \\ 0 & 1 & 0 & 0 \end{bmatrix} \tag{6}$$

The strain–displacement relations can be described in a matrix form as:

$$[\varepsilon] = \begin{bmatrix} \varepsilon_{xx} \\ \gamma_{xz} \end{bmatrix} = \begin{bmatrix} 1 & (z - 4\dfrac{z^3}{3h^2}) & -4\dfrac{z^3}{3h^2} & 0 \\ 0 & 0 & 0 & (1 - 4\dfrac{z^2}{h^2}) \end{bmatrix} \begin{bmatrix} \dfrac{\partial u_0}{\partial x} \\ \dfrac{\partial \Phi_x}{\partial x} \\ \dfrac{\partial^2 w_0}{\partial x^2} \\ \Phi_x + \dfrac{\partial w_0}{\partial x} \end{bmatrix} = [Z]\,[\bar{\varepsilon}] \tag{7}$$

where $[\bar{\varepsilon}]$ is expressed in the following equation:

$$[\bar{\varepsilon}] = \begin{bmatrix} \dfrac{\partial}{\partial x} & 0 & 0 & 0 \\ 0 & 0 & 0 & \dfrac{\partial}{\partial x} \\ 0 & \dfrac{\partial^2}{\partial x^2} & 0 & 0 \\ 0 & 0 & 1 & 1 \end{bmatrix} [\bar{U}] = [d]\,[\bar{U}] \tag{8}$$

So, [ε] can be presented in the following matrix form:

$$[\varepsilon] = [Z]\,[d]\,[\bar{U}] \tag{9}$$

The stress-strain relationship for an FGCNTRC beam is as follows:

$$[\sigma] = [D]\,[\varepsilon] \tag{10}$$

where [σ], [ε], [D] and its components are:

$$[\sigma] = [\sigma_{xx} \quad \sigma_{xz}]^T$$

$$[\varepsilon] = [\varepsilon_{xx} \quad \gamma_{xz}]^T \tag{11}$$

$$[D] = \begin{bmatrix} Q_{11}(z) & 0 \\ 0 & Q_{55}(z) \end{bmatrix} \tag{12}$$

$$Q_{11}(z) = \frac{E(z)}{1-\nu^2} \tag{13}$$

$$Q_{55}(z) = G(z) \tag{14}$$

In this research, the beam is supported by viscoelastic foundation. The Kelvin-Voigt linear model is used for modeling of the viscoelastic foundation. The relationship between force per unit area and deflection in this model can be calculated according to the following equation [67]:

$$P(x,t) = k_w w(x,t) + c_d \frac{\partial w(x,t)}{\partial t} \tag{15}$$

where k_w is the elastic coefficient of the foundation in terms of (N/m^3), and C_d is the damping coefficient of the foundation in terms of (N.s/m^3).

3.2. Finite element model of governing equations

The approximation of the displacement field in each element of the beam is as follows:

$$[\bar{U}^{(e)}(x,t)] = [N(x)]\left[Q^{(e)}(t)\right] \tag{16}$$

$\left[Q^{(e)}(t)\right]$ is nodal degrees of freedom of the beam element and $[N(x)]$ is shape function matrix and its components are shown in the appendix. $\left[Q^{(e)}(t)\right]$ contains u_i, w_i, $\frac{\partial w_i}{\partial x}$ and Φ_i. For u_i and Φ_i, the linear approximation is used and for approximation of w_i and $\frac{\partial w_i}{\partial x}$, the Hermitian element of the Euler-Bernoulli beam is used.

By replacing the equation (16) in (8):

$$[\bar{\varepsilon}] = [B]\left[Q^{(e)}\right] \tag{17}$$

In which [B]=[d] $[N(x)]$ represents the derivative of the matrix of the shape functions in terms of x and is explained in the appendix. The velocity components are obtained from the time derivative of the displacement field as follows:

$$[\dot{\bar{U}}] = [N(x)]\left[\dot{Q}^{(e)}(t)\right] \tag{18}$$

where $\left[\dot{Q}^{(e)}(t)\right]$ is the velocity component of element nodes.

The equation of motion of is extracted by using the Lagrange equations as follows:

$$\left\{\frac{d}{dt}\left(\frac{\partial T}{\partial \dot{Q}}\right)\right\} + \left\{\frac{\partial R}{\partial \dot{Q}}\right\} + \left\{\frac{\partial U}{\partial Q}\right\} = F \tag{19}$$

In the above equation, kinetic energy is a function of the dissipation of the Rayleigh and the total potential energy and the total force on the beam.

The kinetic energy and the total potential energy are defined as follow:

$$T^{(e)} = \frac{1}{2} \iiint [\dot{U}]^T [Z_c]^T \rho(z) \; [Z_c] \; [\dot{U}] \, dx \, dy \, dz$$
$$= \frac{1}{2} \, b \int_0^{l^{(e)}} [\dot{U}]^T \left(\int_{-h/2}^{h/2} [Z_c]^T \rho(z) \; [Z_c] \, dz \right) [\dot{U}] \, dx = \frac{1}{2} \, b \int_0^{l^{(e)}} \left[\dot{Q}^{(e)}\right]^T [N]^T [\bar{Z}] \; [N] \left[\dot{Q}^{(e)}\right] dx \quad (20)$$

Total potential energy of system is as:

$$U^{(e)} = U_1^{(e)} + U_2^{(e)} = \frac{1}{2} \iiint \varepsilon^T \sigma \, dV + \frac{1}{2} \iint k_w w^2 \, dxdy$$
$$= \frac{1}{2} \, b \int_0^{l^{(e)}} \int_{-h/2}^{h/2} \left[Q^{(e)}\right]^T [B]^T [Z]^T \; [D] \; [Z] \; [B] \left[Q^{(e)}\right] dx \, dz + \frac{1}{2} \, b \int_0^{l^{(e)}} \left[Q^{(e)}\right]^T [\bar{N}]^T \, k_w \, [\bar{N}] \left[Q^{(e)}\right] dx \quad (21)$$
$$= \frac{1}{2} \left[Q^{(e)}\right]^T \left(b \int_0^{l^{(e)}} [B]^T [\bar{D}] \; [B] \, dx \right) \left[Q^{(e)}\right] + \frac{1}{2} \left[Q^{(e)}\right]^T \left(b \int_0^{l^{(e)}} [\bar{N}]^T \, k_w \, [\bar{N}] \; dx \right) \left[Q^{(e)}\right]$$

$[\bar{Z}]$ and $[\bar{D}]$ are defined as follow and $\bar{N}$ is presented in appendix:

$$[\bar{D}] = \int_{-\frac{h}{2}}^{\frac{h}{2}} [Z]^T [D] \; [Z] \; dz$$
$$[\bar{Z}] = \int_{-h/2}^{h/2} [Z_c]^T \rho(z) \; [Z_c] \, dz \quad (22)$$

Since the damping of the viscoelastic foundation is a function of the Rayleigh dissipation (R). So, the equation of Rayleigh dissipation matrix for each element of the beam is:

$$R^{(e)} = \frac{1}{2} \iint c_d \; \dot{w}^2 \, dx \, dy =$$
$$\frac{1}{2} \, b \int_0^{l^{(e)}} \left[\dot{Q}^{(e)}\right]^T [\bar{N}]^T c_d \, [\bar{N}] \left[\dot{Q}^{(e)}\right] dx = \frac{1}{2} \left[\dot{Q}^{(e)}\right]^T \left(b \int_0^{l^{(e)}} [\bar{N}]^T c_d \, [\bar{N}] \; dx \right) \left[\dot{Q}^{(e)}\right] \quad (23)$$

If $p_z(t)$ is the external force of the beam, the work performed is defined by equation (24):

$$W_f^{(e)} = \frac{1}{2} \iint \begin{bmatrix} 0 \\ p_z \\ 0 \\ 0 \end{bmatrix} w \; dA = \frac{1}{2} \left[Q^{(e)}\right]^T \left(b \int_0^{l^{(e)}} [\bar{N}]^T \begin{bmatrix} 0 \\ p_z \\ 0 \\ 0 \end{bmatrix} dx \right) \quad (24)$$

Therefore, the mass matrix $[M^{(e)}]$, The stiffness matrix caused by strain $[K_\varepsilon^{(e)}]$, the stiffness matrix due to the elastic properties of the foundation $[K_{kw}^{(e)}]$, the damping matrix due to damping property of foundation $[C^{(e)}]$ and the external force matrix for each element of the beam $\{F^{(e)}\}$ are as following:

$$[M^{(e)}] = b\int_0^{l^{(e)}} [N]^T [\bar{Z}]\, [N]\, dx \tag{25}$$

$$[K_s{}^{(e)}] = b\int_0^{l^{(e)}} [B]^T [\bar{D}]\, [B]\, dx \tag{26}$$

$$[K_{kw}{}^{(e)}] = b\int_0^{l^{(e)}} [\bar{N}]^T\, k_w\, [\bar{N}]\; dx \tag{27}$$

$$[C^{(e)}] = b\int_0^{l^{(e)}} [\bar{N}]^T c_d\, [\bar{N}]\; dx \tag{28}$$

$$\{F^{(e)}\} = b\int_0^{l^{(e)}} [\bar{N}]^T \begin{bmatrix} 0 \\ p_z \\ 0 \\ 0 \end{bmatrix} dx \tag{29}$$

After assembly of element matrices, the matrix form of the Lagrange equations is as:

$$[M]\,[\ddot{Q}] + [C]\,[\dot{Q}] + [K]\,[Q] = \{F\} \tag{30}$$

Finally, Newmark method [68-75] is used to solve the governing equation (35) in time domain.

3. Numerical results

In this research, the dynamic analysis of carbon nanotube-reinforced composite resting on a viscoelastic foundation using finite element methods is presented. In this way, four patterns are considered for the nanotube distributions in the thickness direction. Distributed transverse dynamic force $P = 2e6N/m$ in a period of 0.005 s is applied to the beam, and then removed (See Fig 3). The results obtained by considering Poly Methyl methacrylate as the base material of the beam.

The mechanical property of Poly Methyl methacrylate is considered as the following:

$E_m = 2.5Gpa$, $v_m = 0.3$, $\rho_m = 1190kg/m^3$,

The mechanical property of CNT considered as:

$E_{11}^{cnt} = 5646.6Gpa, E_{22}^{cnt} = 7080Gpa \;\; G_{12}^{cnt} = 1944.5Gpa \;\; v_{12}^{cnt} = 0.175 \;\; \rho_{cnt} = 2100kh/m^3$

3.1. Verification:

In this section, the results of this research are compared with the results of other articles for validation. Since there is no reference for dynamic analysis of FGCNT composite beam on viscoelastic foundation, the results of the present study are validated with the existing results for the free vibration analysis of FGCNT beams with simplification in the present study. For this purpose, in Table 2, the results for the analysis of free vibrations of the FGCNT beam using the third-order shear theory are compared with the results of Ref [58]. The boundary condition of the problem is clamped beam. For comparing the present results with those of Ref [58], the natural frequency must be dimensionless as the following:

$$\bar{\omega} = \frac{\omega L^2}{h}\sqrt{\frac{\rho_m}{E_m}} \tag{31}$$

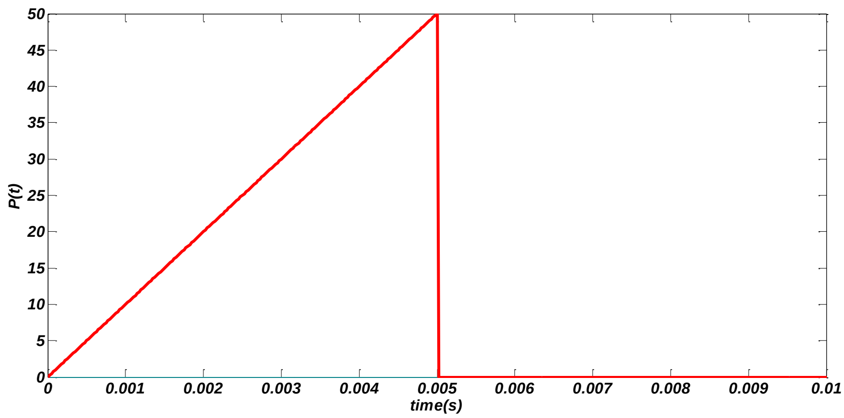

Fig. 3 Time history of impulsive force subjected to beam

Table 2 Fundamental frequency of clamped FGCNT beam for different types of CNTs distribution ($L/h = 10, V_{cnt}^{*} = 0.17$) [58].

PRESENT	[38]	Nanotube distribution
18.4957	18.4950	FGV
19.9297	19.9291	FGX
19.2221	19.2214	FGU

The compression between present result and Ref [58] shows an excellent agreement.

3.2. Transient response of FGCNTRC beam:

In this section, the effect of various factors such as viscoelastic foundation coefficients, CNT pattern through the thickness, volume weight fraction of CNT and geometric parameters on transient displacement and stresses are investigated. The parameters of transverse displacement, normal and shear stress will be dimensionless as the following:

$$\bar{w} = (w_0\ E^m I)/(PL^4) \qquad , I = bh^3/12 \tag{32}$$

$$\overline{\sigma_{xx}} = (\sigma_{xx} bh)/(PL) \tag{33}$$

$$\overline{\sigma_{xz}} = (\sigma_{xz} bh)/(PL) \tag{34}$$

The results are investigated for two different states, surrounded by a viscoelastic foundation (cd = 0.5e5, kw =

1e9) and without foundation and simply supported boundary condition. As can be seen, Figs 4 and 5 shows the effect of different CNT pattern on dimensionless transverse displacement of the mid-point of structure (S-S, L/h=10, V_{cnt}^{*}= 0.17) for with and without foundation. The maximum and minimum amplitude of vibration are related to FG-O and FG-X, respectively. On the other hand, the structure reaches the maximum stiffness in FG-X pattern while FG-O pattern provide lower stiffness.

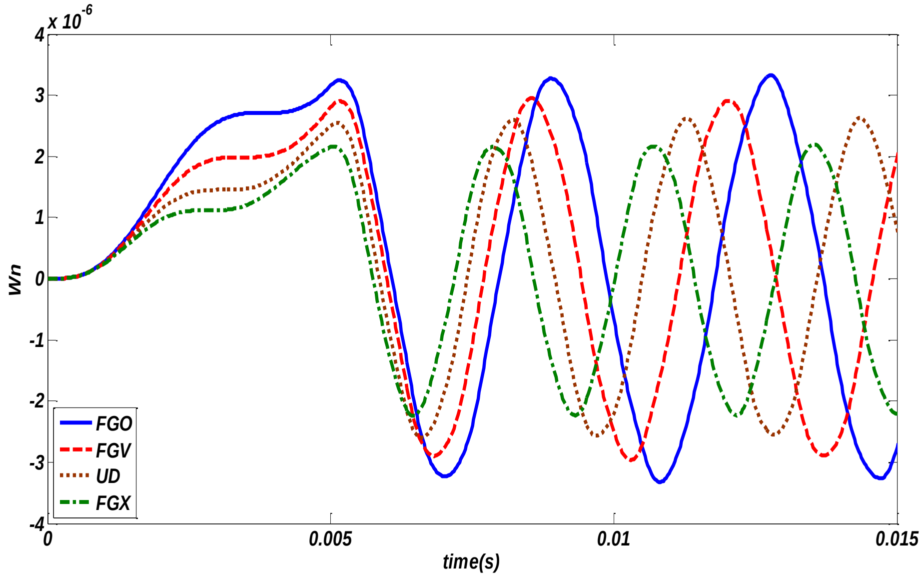

Fig. 4 The effect of different distribution of CNTs on non-dimensional transverse displacement (S-S, L/h=10, V_{cnt}^{*}= 0.17, kw=0, cd=0)

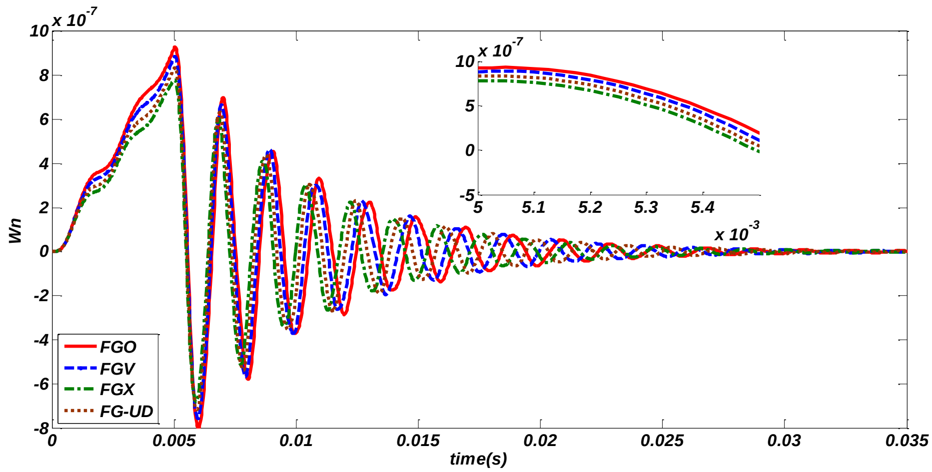

Fig. 5 The effect of different distribution of CNTs on non-dimensional transverse displacement (S-S, L/h=10, V_{cnt}^{*}= 0.17, kw=1e9, cd=0.5e5)

Figs 6 and 7 show the effect of various volume fractions of CNT on the dimensionless transverse displacement of the mid-point of structure (FGV, S-S, L/h=10) for with and without foundation, respectively. By increasing the volume fraction of CNT, the maximum transient deflection of mid-point of the structure considerably decreases (see Fig 5). Also, the maximum amplitude of vibration of the beam decreases by increasing the weight fraction of CNT (see Fig 6).

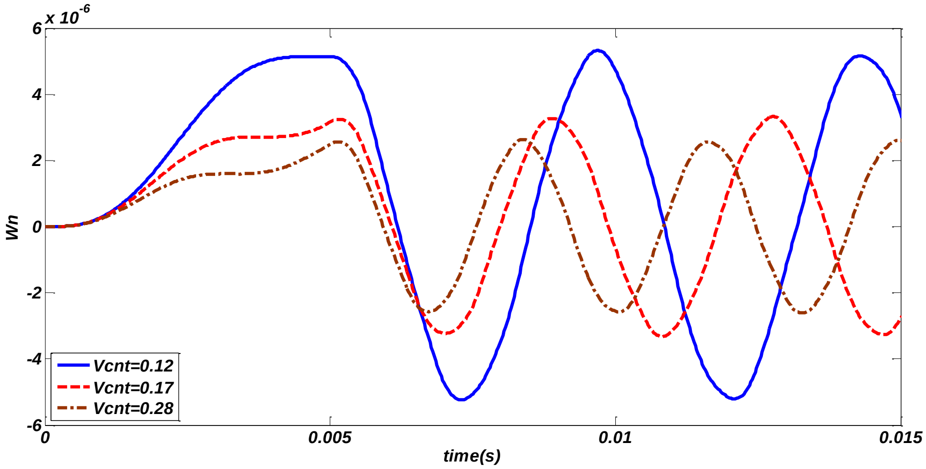

Fig. 6 The effect of different volume fraction of CNTs on non-dimensional transverse displacement (FGV, S-S, L/h=10, kw=0, cd=0)

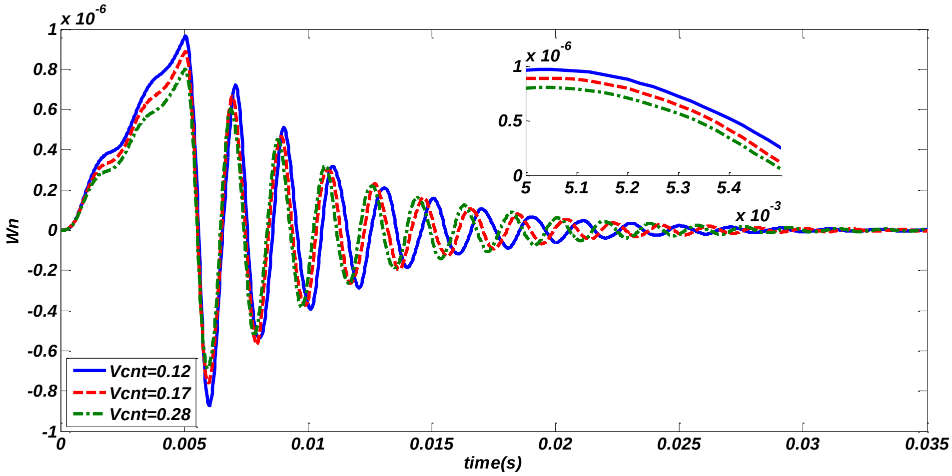

Fig. 7 The effect of different volume fraction of CNTs on non-dimensional transverse displacement (FGV, S-S, L/h=10, kw=1e9, cd=0.5e5)

The effects of slenderness ratio on transverse displacement of midpoint of structure for with and without foundation ((FGV, S-S, $Vcnt^*$= 0.17) are depicted in Figs 8 and 9, respectively. It is obvious that by increasing the slenderness ratio, the stiffness of structure decreases, consequently the deflection of FGNTRC beam increases.

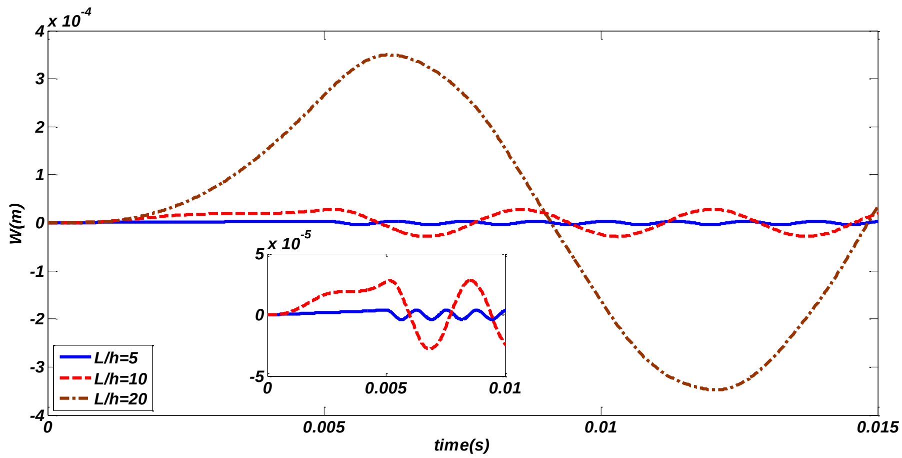

Fig. 8 The effect of slenderness ratio on transverse displacement

(FGV, S-S, $Vcnt^*$= 0.17 kw=0, cd=0)

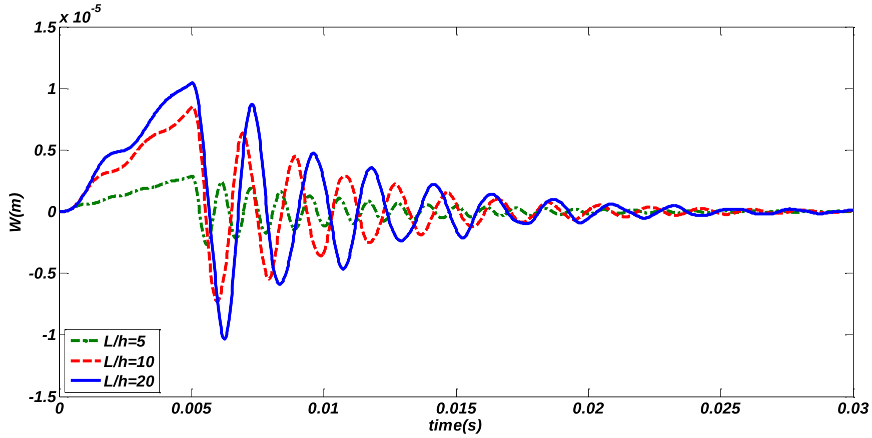

Fig. 9 The effect of slenderness ratio on transverse displacement (FGV, S-S, L/h=10, V_{cnt}^{*}= 0.17, kw=1e9, cd=0.5e5)

Figs 10 and 11 indicate the influence of various CNT patterns on the dimensionless transverse normal and shear stresses of the through the thickness mid-point of beam (FGV, S-S, L/h=10, kw=1e9, cd=0.5e5). The maximum and minimum values of shear stress of beam are related to FG-UD and FG-O, while the maximum and minimum values of normal stresses of the beam do not belong to a specific CNT pattern. For instance, the maximum tension stress is related to FGV, while the maximum compression stress belongs to FGX. For the case that the beam is not supported by viscoelastic foundation, the impact of various CNT distributions on the dimensionless transverse normal and shear stresses of the through the thickness mid-point of the beam are depicted in Figs 12 and 13. It is mentioned that the behavior of normal stress of beam without foundation is as same as when the structure has viscoelastic foundation, while for beam with the viscoelastic foundation, the maximum and minimum shear stresses of the beam are related to FGO and FGV patterns. The influences of volume fraction of CNT on the normal and shear stresses of the mid-point of the structure for beam resting on viscoelastic foundation (unload time=0.005s, V_{cnt}^{*}= 0.17, S-S, L/h=10, kw=1e9, cd=0.5e5) and for beam is not supported on viscoelastic foundation (unload time=0.005s, V_{cnt}^{*}= 0.17, S-S, L/h=10, kw=0, cd=0) are shown in Figs 14 to 17. For both cases, by increasing the volume fraction of CNT, the normal and shear stresses of structure increase. However, by increasing the volume fraction of CNT, normal stresses increase more than shear stresses. On the other hand, the effect of volume fraction of CNT is considerable on normal stress than shear stress of the beam. The time history of normal and shear stresses of mid-point of the structures for different volume fractions of CNT (FGV, S-S, L/h=10, kw=1e9, cd=0.5e5) are reported in Figs18 and 19, respectively. By increasing the volume fraction of CNT, the amplitude of stresses raises. The influence of stiffness of foundation on transient deflection of midpoint of the beam is shown in Fig 20 (FGV, S-S, L/h=10, V_{cnt}^{*}=0.17, cd=0.5e5). By increasing the stiffness of foundation the transient deflection considerably decreases. The effect of different damping coefficient of foundation on the non-dimensional transverse displacement (FGV, S-S, L/h=10, V_{cnt}^{*}=0.17) is depicted in Fig 21. As it can be seen from these figures, by increasing damping of the foundation, amplitude of vibration decreases and vibration of beam can be seen in three situations such as under-damped, critically-damped and over-damped.

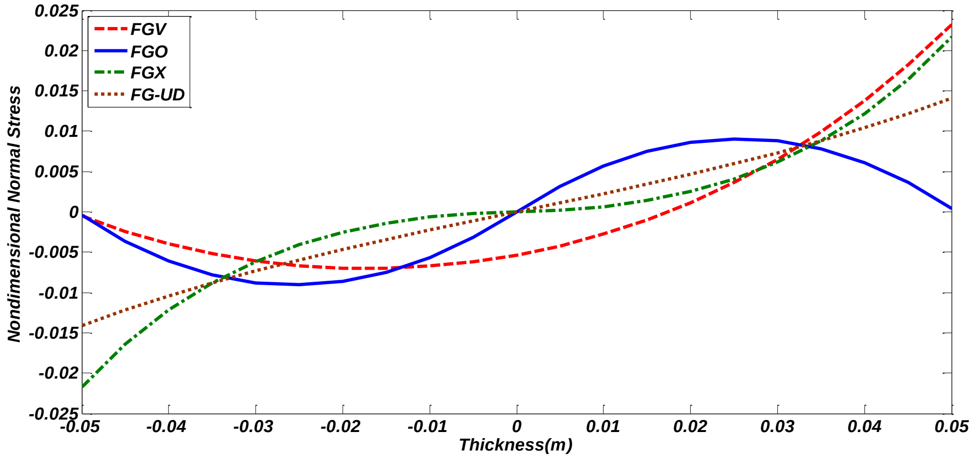

Fig. 10 The effect of different distribution of CNTs on non-dimensional normal stress through the thickness of beam (unload time=0.005s, V_{cnt}^{*}= 0.17, S-S, L/h=10, kw=1e9, cd=0.5e5)

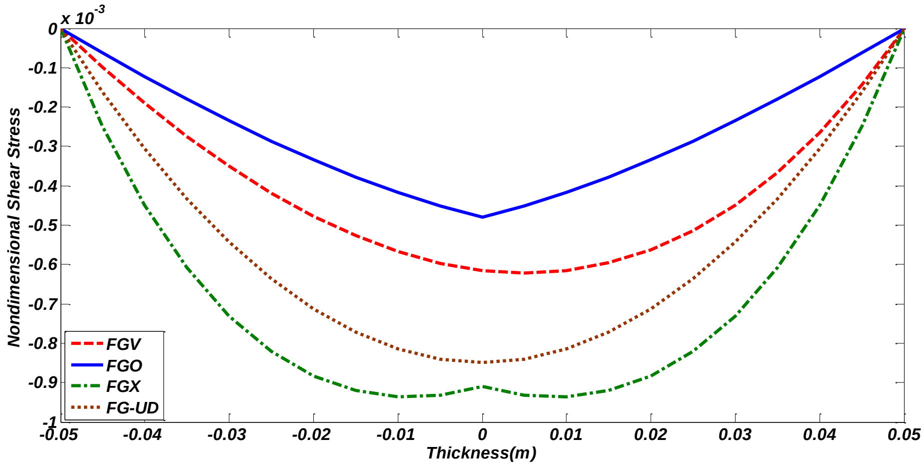

Fig. 11 The effect of different distribution of CNTs on non-dimensional shear stress through the thickness of beam (unload time=0.005s, V_{cnt}^{*}= 0.17, S-S, L/h=10, kw=1e9, cd=0.5e5)

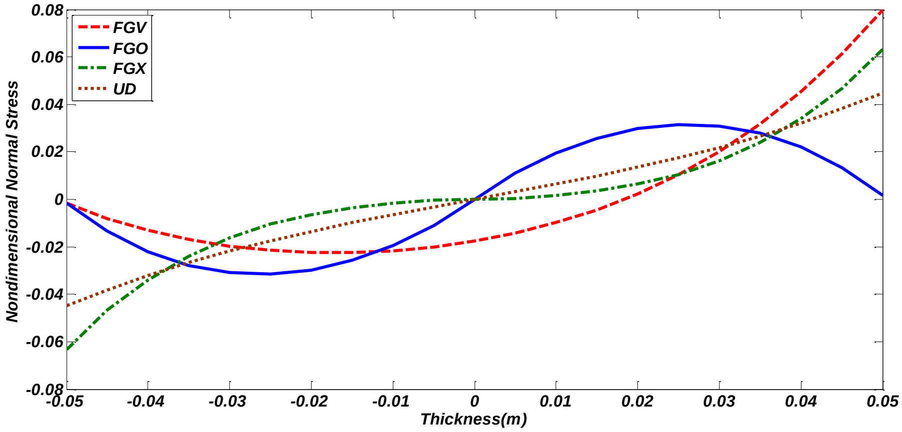

Fig. 12 The effect of different distribution of CNTs on non-dimensional normal stress through the thickness of beam (unload time=0.005s, V_{cnt}^{*}= 0.17, S-S, L/h=10, kw=0, cd=0)

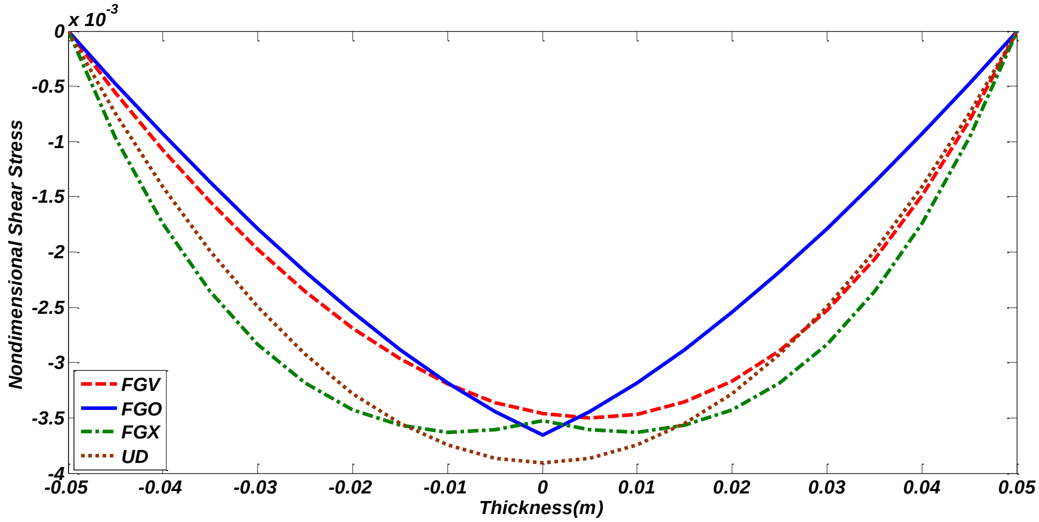

Fig. 13 The effect of different distribution of CNTs on non-dimensional shear stress through the thickness of beam (unload time=0.005s, V_{cnt}^{*}= 0.17, S-S, L/h=10, kw=0, cd=0)

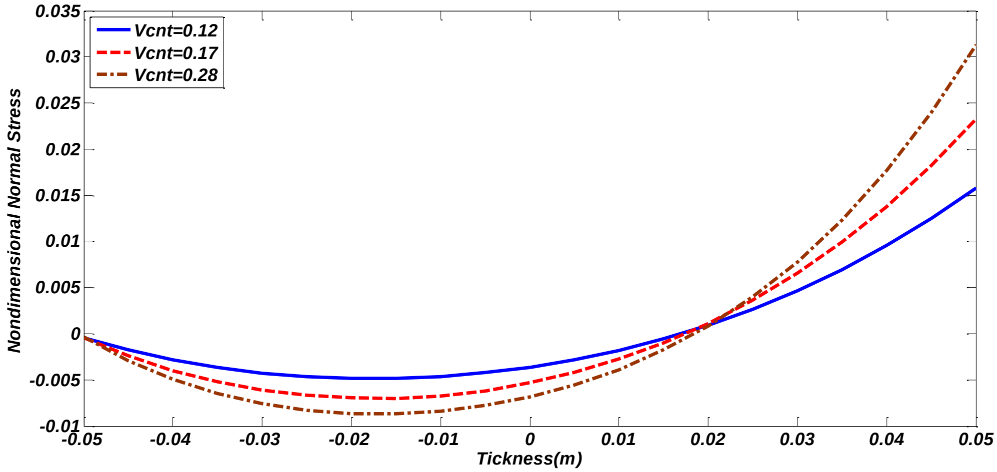

Fig. 14 The effect of different volume fraction of CNT on non-dimensional normal stress through the thickness of beam (unload time=0.005s,FG-V, S-S, L/h=10, kw=1e9, cd=0.5e5)

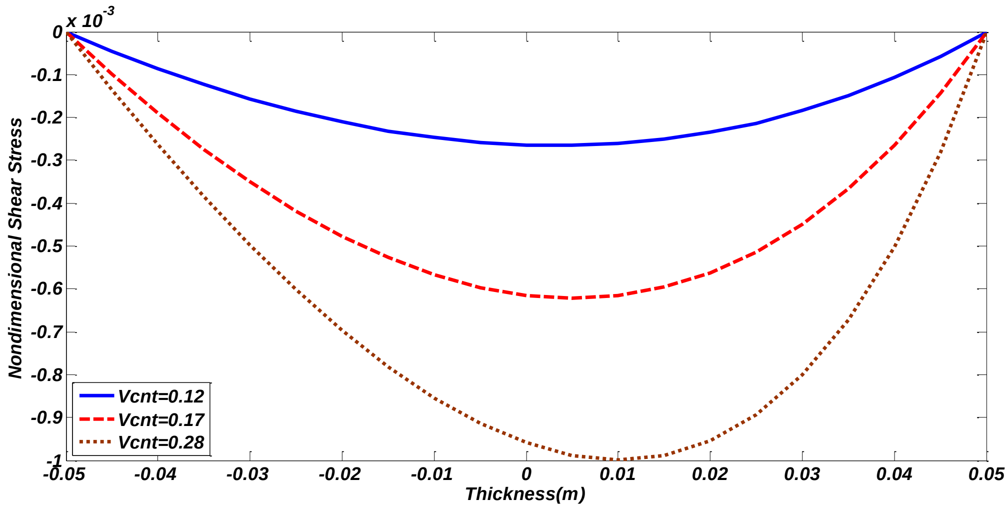

Fig. 15 The effect of different volume fraction of CNT on non-dimensional shear stress through the thickness of beam (unload time=0.005s,FG-V, S-S, L/h=10, kw=1e9, cd=0.5e5)

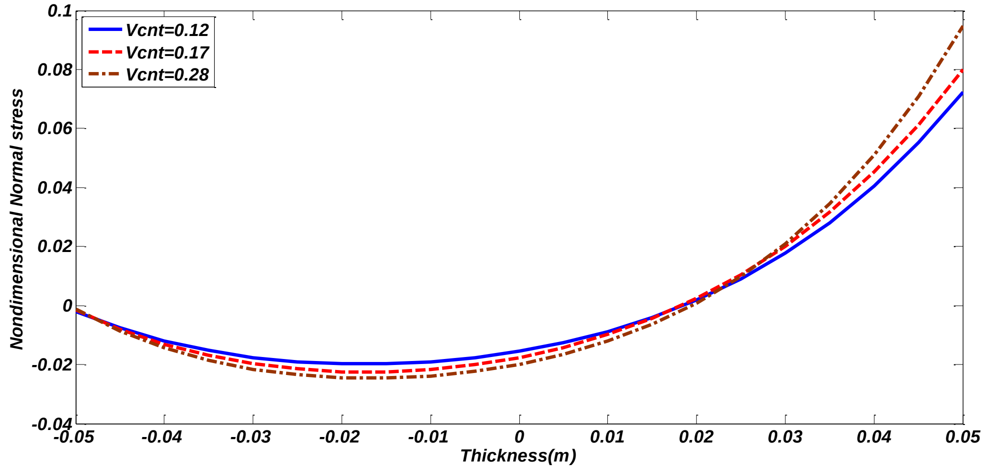

Fig. 16 The effect of different volume fraction of CNT on non-dimensional normal stress through the thickness of beam
(unload time=0.005s, , $V_{cnt}^* = 0.17$, S-S, L/h=10, kw=0, cd=0)

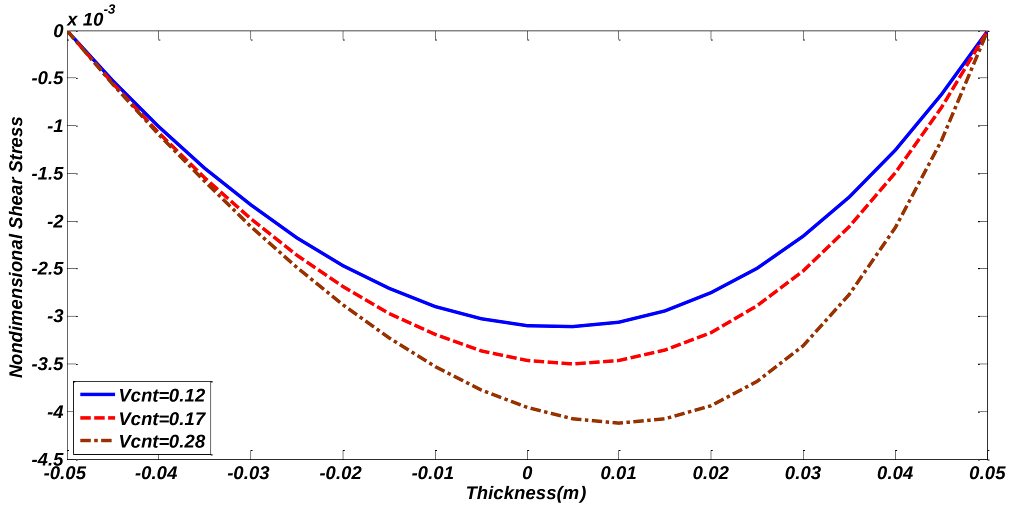

Fig. 17 The effect of different volume fraction of CNT on non-dimensional shear stress through the thickness of beam
(unload time=0.005s, V_{cnt}^*= 0.17, S-S, L/h=10, kw=0, cd=0)

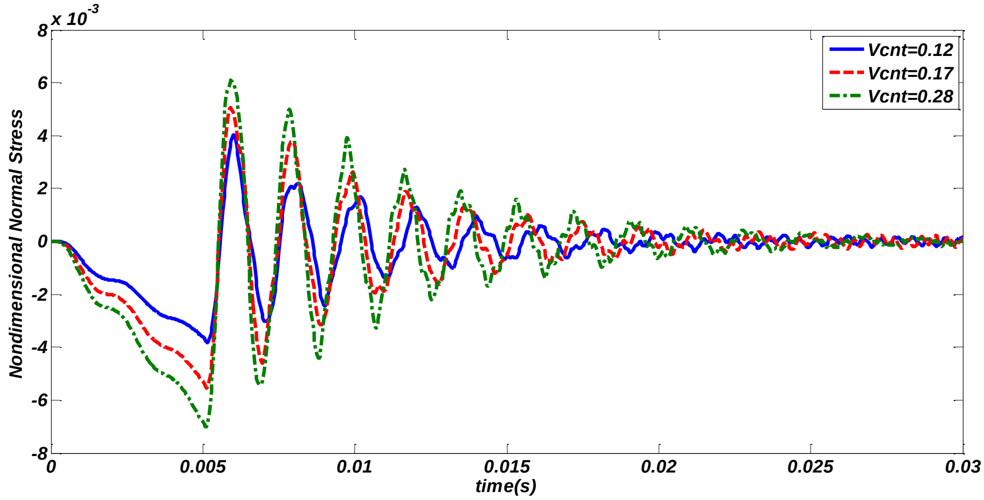

Fig. 18 The effect of different volume fraction of CNT on non-dimensional normal stress (FGV, S-S, L/h=10, kw=1e9, cd=0.5e5)

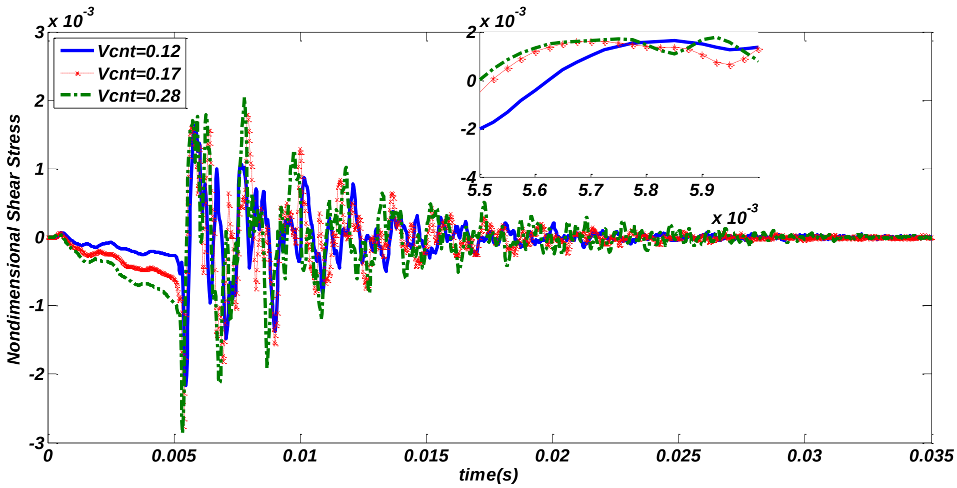

Fig. 19 The effect of different volume fraction on of CNT non-dimensional shear stress (FGV, S-S, L/h=10, kw=1e9, cd=0.5e5)

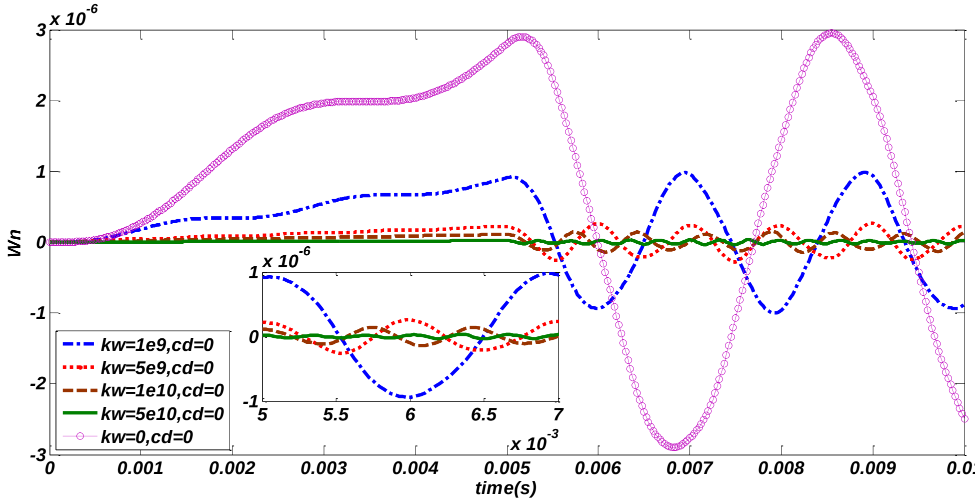

Fig. 20 The effect of different elastic coefficient of foundation on non-dimensional transverse displacement (FGV, S-S, L/h=10, V_{cnt}^{*}=0.17)

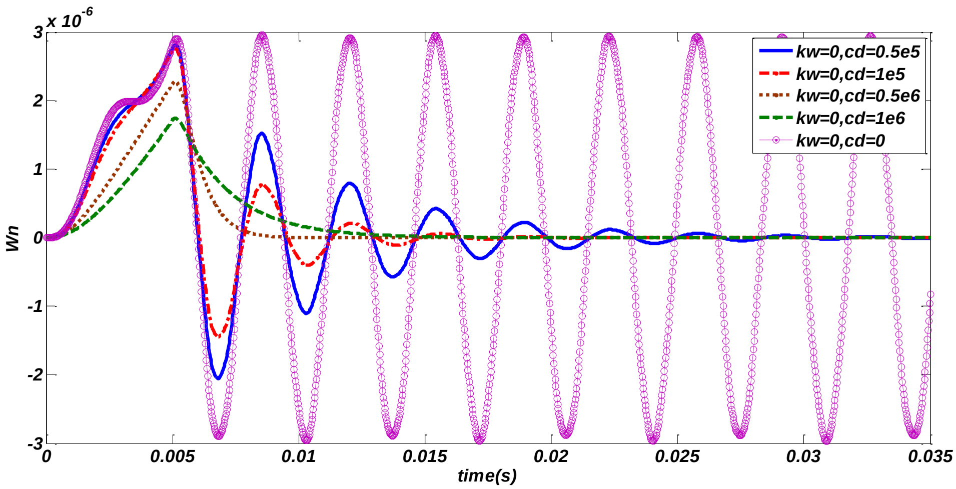

Fig. 21 The effect of different damping coefficient of foundation on non-dimensional transverse displacement (FGV, S-S, L/h=10, V_{cnt}^{*}= 0.17)

4. Conclusion

In this paper, dynamic response of FG-CNT reinforced composite beams resting on a viscoelastic foundation based on higher-order shear deformation theory in conjunction with FEM and Lagrange approach is investigated. The results show that in FG-O pattern, the stiffness of the structure is less than the other patterns and this distribution has the highest amount of displacement and amplitude of vibration. Also, by decreasing the volume weight fraction of CNT, the amplitude of vibration increases. Also, by increasing the volume weight fraction of CNT, the values of normal and shear stresses along the thickness increase. By applying viscoelastic foundation, the values of stresses significantly decrease. The results show that in the presence of the foundation, the lowest shear stress is related to the FG-O pattern and the highest shear stress is related to the FGX distribution. However, for the case of without foundation, the highest shear stress is related to the UD pattern and the lower shear stress is related to the FG-V distribution. Finally, by increasing the elastic coefficient of the foundation, the amplitude of vibration of the beam considerably decreases, and the frequency of the vibrations increases.

References

[1] G. Shi, K. Y. Lam, Finite Element Vibration Analysis of Composite Beams Based on higher-order Beam Theory, *Journal of Sound and Vibration*, Vol. 219, No. 4, pp. 707-721, 1999.

[2] B. V. Sankar, An elasticity solution for functionally graded beams, *Composites Science and Technology*, Vol. 61, No. 5, pp. 689–696, 2001.

[3] Y. H. Chen, Y. H. Hung, Response of an infinite Timoshenko beam on a viscoelastic foundation to a harmonic moving load, *Journal of Sound and Vibration*, Vol. 241, No. 5, pp. 809-824, 2001.

[4] A. Chakraborty, S. Gopalakrishnan, J. N. Reddy, A new beam finite element for the analysis of functionally, *International Journal of Mechanical Sciences*, Vol. 45, No. 3, pp. 519-539, 2003.

[5] M. H. Kargarnovin, D. Younesian, Dynamics of Timoshenko beams on Pasternak foundation under moving load, *Mechanics Research Communicatins*, Vol. 31, No. 6, pp. 713-723, 2004.

[6] J. Yang, Y. Chen, Y. Xiang, X.L. Jia, Free and forced vibration of cracked inhomogeneous beams, *Journal of Sound and Vibration*, vol 312, No. 1, pp. 166-181, 2008.

[7] R. Kadoli, K. Akhtar, N. Ganesan, Static analysis of functionally graded beams using higher order shear deformation theory, *Applied Mathematical Modelling*, Vol. 32, No.12, pp. 2509–2525, 2008.

[8] J. Ying, C. F. Lu, W. Q. Chen, Two-dimensional elasticity solutions for functionally graded beams resting on elastic foundations, *Composite Structures*, Vol 84, No. 3, pp. 209–219, 2008.

[9] F. F. Calım, Dynamic analysis of beams on viscoelastic foundation, *European Journal of Mechanics A/Solids*, Vol. 28, No. 3, pp. 469–476, 2009.

[10] M. Simsek, T. Kocatürk, Free and forced vibration of a functionally graded beam subjected to a concentrated moving harmonic load, *Composite Structures*, Vol. 90, No. 4, pp. 465–473, 2009.

[11] M. Simsek, Non-linear vibration analysis of a functionally graded Timoshenko beam, under action of a moving harmonic load, *Composite Structures*, Vol 92, No. 10, pp. 2532–2546, 2010.

[12] S. khalili, S. A. Eftekhari, A mixed Ritz-DQ method for forced vibration of functionally graded beams carrying moving loads, *Composite Structures*, Vol. 92, No. 10, pp. 2497-2511, 2010.

[13] S. R. Mohebpour, A. R. Fiouz, A. A. Ahmadzadeh, Dynamic investigation of laminated composite beams with shear and rotary inertia effect subjected to the moving oscillators using FEM, *Composite Structures*, Vol 93, No. 3, pp. 1118–1126, 2011.

[14] K. K. Pradhan, S. Chakraverty, Free vibration of Euler and Timoshenko functionally graded beams by Rayleigh–Ritz method, *Composites*, Vol. B51, pp. 175–184, 2013.

[15] S. M. Abdelghany, K. M. Ewis, A. A. Mahmoud, M. M. Nassar, Dynamic response of non-uniform beam subjected to moving load and resting on non-linear viscoelastic foundation, *Journal of Basic Applied Science*, Vol. 4, No. 3, pp. 192-199, 2015.

[16] F. Kiarasi, M. Babaei, R. Dimitri, F. Tornabene, Hygrothermal modeling of the buckling behavior of sandwich plates with nanocomposite face sheets resting on a Pasternak foundation. *Continuum Mechanics and Thermodynamics*, Vol. 33, No. 4, pp. 911-932, 2021.

[17] K. T. Lau, C. Gu, G. H. Gao, H. Y. Ling, S. R. Reid, Stretching process of single- and multi-walled carbon nanotubes for nanocomposite applications, *Carbon*, Vol. 42, No. 2, pp. 426-428, 2004.

[18] A. M. K. Esawi, M. M. Farag, Carbon nanotube reinforced composites: potential and current challenges, *Material and Design*, Vol. 28, No. 9, pp. 2394-2401, 2007.

[19] F. Kiarasi, M. Babaei, P. Sarvi, K. Asemi, M. Hosseini, M. Omidi Bidgoli, A review on functionally graded porous structures reinforced by graphene platelets. *Journal of Computational Applied Mechanics*, Vol. 52, No. 4, pp. 731-750, 2021.

[20] F. Kiarasi, M. Babaei, M. Mollaei, S. M. Mohammadi, K. Asemi, Free vibration analysis of FG porous joined truncated conical-cylindrical shell reinforced by graphene platelets. *Advances in nano research*, Vol. 11, No. 4, pp. 361-380, 2021.

[21] M. M. Adeli, A. Hadi, M. Hosseini, H. H. Gorgani, Torsional vibration of nano-cone based on nonlocal strain gradient elasticity theory, *The European Physical Journal Plus*, Vol. 132, pp. 393, 2017.

[22] A. Barati, A. Hadi, M. Z. Nejad, R. Noroozi, On vibration of bi-directional functionally graded nanobeams under magnetic field, *Mechanics Based Design of Structures and Machines*, pp. 1-18, 2020.

[23] A. Barati, M. Mousavi Khoram, M. Shishesaz, M. Hosseini, Size-dependent thermoelastic analysis of rotating nanodisks of variable thickness, *Journal of Computational Applied Mechanics,* Vol. 51, pp. 340-360, 2020.

[24] A. Hadi, M. Z. Nejad, M. Hosseini, Vibrations of three-dimensionally graded nanobeams, *International Journal of Engineering Science,* Vol. 128, pp. 12-23, 2018.

[25] A. Hadi, M. Z. Nejad, A. Rastgoo, M. Hosseini, Buckling analysis of FGM Euler-Bernoulli nano-beams with 3D-varying properties based on consistent couple-stress theory, *Steel and Composite Structures,* Vol. 26, pp. 663-672, 2018.

[26] H. Haghshenas Gorgani, M. Mahdavi Adeli, and M. Hosseini, Pull-in behavior of functionally graded micro/nano-beams for MEMS and NEMS switches, *Microsystem Technologies*, vol. 25, pp. 3165-3173, 2019.

[27] M. Hosseini, M. Shishesaz, A. Hadi, Thermoelastic analysis of rotating functionally graded micro/nanodisks of variable thickness, *Thin-Walled Structures*, Vol. 134, pp. 508-523, 2019.

[28] M. Hosseini, M. Shishesaz, K. N. Tahan, A. Hadi, Stress analysis of rotating nano-disks of variable thickness made of functionally graded materials," *International Journal of Engineering Science*, Vol. 109, pp. 29-53, 2016.

[29] M. Shahsavari, K. Asemi, M. Babaei, F. Kiarasi, Numerical investigation on thermal post-buckling of annular sector plates made of FGM via 3D finite element method. *Mechanics of Advanced Composite Structures*, Vol. 8, No. 2, pp. 309-320, 2021.

[30] M. Babaei, F. Kiarasi, S. M. Hossaeini Marashi, M. Ebadati, F. Masoumi, K. Asemi, Stress wave propagation and natural frequency analysis of functionally graded graphene platelet-reinforced porous joined conical–cylindrical–conical shell. *Waves in Random and Complex Media*, pp. 1-33, 2021.

[31] H. Nazari, M. Babaei, F. Kiarasi, K. Asemi, Geometrically nonlinear dynamic analysis of functionally graded material plate excited by a moving load applying first-order shear deformation theory via generalized differential quadrature method. *SN Applied Sciences*, Vol. 3, No. 11, pp. 1-32, 2021.

[32] M. M. Khoram, M. Hosseini, A. Hadi, M. Shishehsaz, Bending Analysis of Bidirectional FGM Timoshenko Nanobeam Subjected to Mechanical and Magnetic Forces and Resting on Winkler–Pasternak Foundation, *International Journal of Applied Mechanics*, Vol. 12, pp. 2050093, 2020.

[33] R. Mahmoudi, A. Barati, M. Hosseini, A. Hadi, Torsional Vibration of Functionally Porous Nanotube Based on Nonlocal Couple Stress Theory, *International Journal of Applied Mechanics*, Vol. 13, No. 10, pp. 2150122, 2021.

[34] M. Mohammadi, M. Hosseini, M. Shishesaz, A. Hadi, A. Rastgoo, Primary and secondary resonance analysis of porous functionally graded nanobeam resting on a nonlinear foundation subjected to mechanical and electrical loads, *European Journal of Mechanics - A/Solids*, Vol. 77, pp. 103793, 2019.

[35] M. Z. Nejad, A. Hadi, Non-local analysis of free vibration of bi-directional functionally graded Euler–Bernoulli nano-beams, *International Journal of Engineering Science,* Vol. 105, pp. 1-11, 2016.

[36] M. Z. Nejad, A. Hadi, A. Rastgoo, Buckling analysis of arbitrary two-directional functionally graded Euler–Bernoulli nano-beams based on nonlocal elasticity theory, *International Journal of Engineering Science,* Vol. 103, pp. 1-10, 2016

[37] M. Shishesaz, M. Hosseini, Mechanical Behavior of Functionally Graded Nano-Cylinders Under Radial Pressure Based on Strain Gradient Theory, *Journal of Mechanics,* Vol. 35, pp. 441-454, 2018.

[38] M. Shishesaz, M. Hosseini, K. Naderan Tahan, A. Hadi, Analysis of functionally graded nanodisks under thermoelastic loading based on the strain gradient theory, *Acta Mechanica*, Vol. 228, pp. 4141-4168, 2017.

[39] A. P. Praveen, V. Rajamohan, A. T. Mathew, Recent developments in investigation on buckling and post buckling responses of laminated composite shells. Polymer Composites, Vol. 39, No. 12, pp. 4231-4242, 2018.

[40] D. T. Dong, V. H. Nam, N. T. Phuong, L. N. Ly, V. M. Duc, N. Van Tien, P. H. Quan, An analytical approach of nonlinear buckling behavior of longitudinally compressed carbon nanotube-reinforced (CNTR) cylindrical shells with CNTR stiffeners in thermal environment. ZAMM-Journal of Applied Mathematics and Mechanics/Zeitschrift für Angewandte Mathematik und Mechanik, e202100228, 2021.

[41] P. T. Hieu, H. Van Tung, Buckling of shear deformable FG-CNTRC cylindrical shells and toroidal shell segments under mechanical loads in thermal environments. ZAMM-Journal of Applied Mathematics and Mechanics/Zeitschrift für Angewandte Mathematik und Mechanik, Vol. 100, No. 11, e201900243, 2020.

[42] M. Babaei, K. Asemi, Static, dynamic and natural frequency analyses of functionally graded carbon nanotube annular sector plates resting on viscoelastic foundation. *SN Applied Sciences*, Vol. 2, No. 10, pp. 1-21, 2020.

[43] M. Hosseini, H. H. Gorgani, M. Shishesaz, and A. Hadi, Size-Dependent Stress Analysis of Single-Wall Carbon Nanotube Based on Strain Gradient Theory, *International Journal of Applied Mechanics,* Vol. 09, pp. 1750087, 2017.

[44] K. M. Liew, Z. X. Lei, L. W. Zhang, Mechanical analysis of functionally graded carbon nanotube

reinforced composites: a review. *Composite Structures*, Vol. 120, pp. 90-97, 2015.

[45] B. Fiedler, F. H. Gojny, M. H. G. Wichmann, M. C. M. Nolte, K. Schulte, Fundamental aspects of nano-reinforced composites, *Composites science and technology*, Vol. 66, No. 16, pp. 3115-3125, 2006.

[46] S. Ahmad, D. Kia, H. Amin, N. Mohamad Hasan, Effect of out-of-plane defects on the postbuckling behavior of graphene sheets based on nonlocal elasticity theory, *Steel and Composite Structures, An International Journal*, Vol. 30, pp. 517-534, 2019.

[47] M. Najafzadeh, M. M. Adeli, E. Zarezadeh, A. Hadi, Torsional vibration of the porous nanotube with an arbitrary cross-section based on couple stress theory under magnetic field, *Mechanics Based Design of Structures and Machines*, Vol. 50, pp. 726-740, 2022.

[48] G. R. Liu, A step-by-step method of rule-of-mixture of fiber-and particle-reinforced composite materials. *Composite structures*, Vol. 40, No, 3-4, pp. 313-322, 1997.

[49] N. Bendenia, M. Zidour, A. A. Bousahla, F. Bourada, A. Tounsi, K. H. Benrahou, A. Tounsi, Deflections, stresses and free vibration studies of FG-CNT reinforced sandwich plates resting on Pasternak elastic foundation. *Computers and Concrete, An International Journal*, Vol. 26, No. 3, pp. 213-226, 2020.

[50] Kiani, Y. Thermal post-buckling of FG-CNT reinforced composite plates. *Composite Structures*, Vol. 159, pp. 299-306, 2017.

[51] J. Wuite, S. Adali, Deflection and Stress behavior of nanocomposite reinforced beams using multiscale analysis, *Composite Structures*, Vol. 71, No. 3, pp. 388-396, 2005.

[52] T. Vodenitcharova, L. C. Zhang, Bending and local buckling of a nanocomposite beam reinforced by a single-walled carbon nanotube, *International journal of solids and structures*, Vol. 43, No. 10, pp. 3006-3024, 2006

[53] Ke LL, Yang J, Kitipornchai S. Nonlinear free vibration of functionally graded carbon nanotube-reinforced composite beams, *Composite Structure*,Vol. 92, No. 3, pp. 676-683, 2010.

[54] M. H. Yas, M. Heshmati, Dynamic analysis of functionally graded nanocomposite beam reinforced by randomly oriented carbon nanotube under the action of moving load, *Applied Mathematical Modelling*, Vol. 36, No. 4, pp. 1371-1394, 2012.

[55] H. S. Shen, Y. Xiang, Nonlinear analysis of nanotube-reinforced composite beams resting on elastic foundations in thermal environments, *Engineering Structures*, Vol. 56, pp. 698-708, 2013.

[56] L. L. Ke, J. Yang, S. Kitipornchai, Dynamic stability of functionally graded carbon nanotube-reinforced composite beams, *Mechanics of Advanced Materials and Structures*, Vol. 20, No. 1, pp. 28-37, 2013.

[57] R. Ansari, M. Faghih Shojaei, V. Mohammadi, R. Gholami, F. Sadeghi, Nonlinear force vibration analysis of functionally graded carbon nanotube-reinforced composite Timoshenko beams, *Composite Structures*, Vol. 113, pp. 316-327, 2014.

[58] F. Lin, Y. Xiang, Vibration of carbon nanotube reinforced composite beams based on the first and third order beam theories, *Applied Mathematical Modelling*, Vol. 38, No. 15, pp. 3741-3754, 2014.

[59] V. K. Chaudhari, A. Lal, Nonlinear free vibration analysis of elastically supported nanotube- reinforced composite beam in thermal environment, *Procedia Engineering*, Vol. 144, pp. 928 – 935, 2016.

[60] R. Zerrouki, A. Karas, M. Zidour, A. A. Bousahla, A. Tounsi, F. Bourada, S. R. Mahmoud, Effect of nonlinear FG-CNT distribution on mechanical properties of functionally graded nano-composite beam. *Structural Engineering and Mechanics*, Vol. 78, No. 2, pp. 117-124, 2021.

[61] L. W. Zhang, Z. X. Lei, K. Liew, Buckling analysis of FG-CNT reinforced composite thick skew plates using an element-free approach. *Composites Part B: Engineering*, Vol. 75, pp. 36-46, 2015.

[62] F. Ebrahimi, M. R. Barati, Thermal buckling analysis of size-dependent FG nanobeams based on the third-order shear deformation beam theory. *Acta Mechanica Solida Sinica*, Vol. 29, No. 5, pp. 547-554, 2016.

[63] A. J. M. Ferreira, C. M. C. Roque, P. A. L. S. Martins, Radial basis functions and higher-order shear deformation theories in the analysis of laminated composite beams and plates. *Composite structures*, Vol. 66, No. 1-4, pp. 287-293, 2014.

[64] R. M. Jones, *Mechanics of composite materials*. CRC press, 2018.

[65] M. Babaei, K. Asemi, P.Safarpour, Natural frequency and dynamic analyses of functionally graded saturated porous beam resting on viscoelastic foundation based on higher order beam theory. *Journal of Solid Mechanics*, Vol. 11, No. 3, pp. 615-634, 2019.

[66] M.Babaei, K. Asemi, P. Safarpour, Buckling and static analyses of functionally graded saturated porous thick beam resting on elastic foundation based on higher order beam theory. *Iranian Journal of Mechanical Engineering Transactions of the ISME*, Vol. 20, No. 1, pp. 94-112, 2019.

[67] A. D. Kerr, Elastic and viscoelastic foundation models, 1964.

[68] K. Asemi, M. Babaei, F. Kiarasi, Static, natural frequency and dynamic analyses of functionally graded porous annular sector plates reinforced by graphene platelets. *Mechanics Based Design of Structures and Machines*, pp. 1-29, 2020.

[69] M. Babaei, K. Asemi, F. Kiarasi, Dynamic analysis of functionally graded rotating thick truncated cone made of saturated porous materials. *Thin-Walled Structures*, Vol. 164, pp. 107852, 2021.

[70] O. Bourihane, Y. Hilali, K. Mhada, Nonlinear dynamic response of functionally graded material plates using a high-order implicit algorithm. *ZAMM-Journal of Applied Mathematics and Mechanics/Zeitschrift für Angewandte Mathematik und Mechanik*, Vol. 100, No. 12, e202000087, 2020.

[71] S. Pandey, S. Pradyumna, Thermal shock analysis of functionally graded sandwich curved beams using a new layerwise theory. *ZAMM-Journal of Applied Mathematics and Mechanics/Zeitschrift für Angewandte Mathematik und Mechanik*, e202100020, 2021.

[72] M. Shariati, M. Shishesaz, R. Mosalmani, S. A. Seyed Roknizadeh, M. Hosseini, Nonlocal effect on the axisymmetric nonlinear vibrational response of nano-disks using variational iteration method, *Journal of Computational Applied Mechanics*, Vol. 52, pp. 507-534, 2021.

[73] I. Eshraghi, S. Dag, Forced vibrations of functionally graded annular and circular plates by domain-boundary element method. *ZAMM-Journal of Applied Mathematics and Mechanics/Zeitschrift für Angewandte Mathematik und Mechanik*, Vol. 100, No. 8, e201900048, 2020.

[74] R. Damghanian, K. Asemi, M. Babaei, A new beam element for static, free and forced vibration responses of microbeams resting on viscoelastic foundation based on modified couple stress and third-order beam theories. *Iranian Journal of Science and Technology, Transactions of Mechanical Engineering*, pp. 1-17, 2020.

[75] M. Babaei, M. H. Hajmohammad, K. Asemi, Natural frequency and dynamic analyses of functionally graded saturated porous annular sector plate and cylindrical panel based on 3D elasticity. *Aerospace Science and Technology*, Vol. 96, pp. 105524, 2020.